Analytical Methods

Detection of PETN and RDX Using a FRET- based Fluorescence Sensor System

Journal:	*Analytical Methods*
Manuscript ID:	AY-ART-02-2015-000416.R1
Article Type:	Paper
Date Submitted by the Author:	03-Apr-2015
Complete List of Authors:	Cyriac, Jobin; Indian Institute of Space Science and Technology, Chemistry Ganiga, Manjunatha; Indian Institute of Space Science and Technology, Chemistry

Detection of PETN and RDX Using a FRET- based Fluorescence Sensor System

Manjunatha Ganiga and Jobin Cyriac*

Department of Chemistry, Indian Institute of Space Science and Technology

Thiruvananthapuram – 695 547, INDIA

*To whom correspondence should be addressed, e-mail: jobincyriac@iist.ac.in

Prepared for publication in *Analytical Methods*

Correspondence to:

Jobin Cyriac
Department of Chemistry
Indian Institute of Space Science and Technology (IIST)
Valiamala P.O.
Thiruvananthapuram
Kerala – 695 547, INDIA

Key Words: Explosive detection, Förster resonance energy transfer (FRET), pentaerythritol tetranitrate (PETN), CdS quantum dots

Abstract

Most of the fluorescence based detection of explosives involves the detection of nitro-aromatic compounds, such as trinitrotoluene (TNT) and dinitrotoluene (DNT). Here, we report a Förster resonance energy transfer (FRET)-based nanosensor system for the highly selective detection of powerful explosives, such as PETN (pentaerythritol tetranitrate) and RDX (cyclotrimethylenetrinitramine). The nanosensor system was composed of cadmium sulfide quantum dots (CdS QDs) and diphenylamine (DPA). Initially, the inherent fluorescence of DPA was quenched by resonance energy transfer to the CdS QDs. During detection, due to the strong interaction of DPA with nitroester or nitramine, the FRET was turned-off and was accompanied by the recovery of the donor's (DPA) fluorescence. This provides an opportunity to follow the detection in a two-way manner, either the decrease in the FRET intensity at ~585 nm or the evolution of fluorescence at ~355 nm. The detection limits for PETN and RDX were found to be 10 nM and 20 nM, respectively. The fluorescence lifetime measurements confirmed that the energy transfer process is effective in the CdS QD-DPA sensor system. The details of the molecular interactions, between QD-DPA and DPA-analyte, were established using infrared spectroscopy. The easy one pot synthesis method of CdS QDs, use of readily available chemicals, excellent selectivity and very good sensitivity make the present sensor system attractive.

---

†Electronic Supporting Information (ESI) available: Additional figures and calculations are available as stated in the text.

Introduction

Accurate and reliable detection of explosives is very important as the world faces continuous threats from terrorism. High explosives such as PETN (pentaerythritol tetranitrate) and RDX (cyclotrimethylenetrinitramine) are the commonly used plastic explosives. Methods for selective detection of trace amounts of these explosives are in demand for security and safety. Analytical methods that have been used for the detection of nitro-aromatic explosives include mass spectrometry (MS),[1] ion mobility spectrometry (IMS),[2, 3] surface enhanced Raman scattering (SERS),[4, 5] colorimetric analysis,[6-8] and electrochemical[9] sensing tools. Mass spectrometry (MS) based on various desorption/ionization methods has been reported for the detection of trace amounts of explosives on a variety of surfaces.[10, 11] While having good sensitivity and selectivity, the cost and need of expertise are the main disadvantages of the MS methods. IMS-based detection is used in airport security and field detection of chemical weapons.[12] IMS mostly relies on vapor detection of the analytes and shows poor selectivity. SERS shows good detection limits, but reproducibility is highly dependent on the substrates.[13] Colorimetric methods

offer convenient visual detection but require specially synthesized receptor molecules. Poor sensitivity is another disadvantage of this method.[7] Sensitivity and pre-concentration steps are the main limitations of some of the reported electrochemical methods.[5] As discussed, many of the aforementioned methods suffer regarding cost, lack of reproducibility and poor selectivity.

Because of their high sensitivity, operational simplicity and potential for portability, fluorescence techniques for the detection of trace chemicals are attractive.[14, 15] However, explosive compounds are not inherently fluorescent and need to overcome this drawback by the reaction of these compounds or their fragments to form fluorescent products.[16-19] Alternatively, by indirect methods, fluorescence of the probe system can be quenched by the explosives. Recently, it was reported that fluorescent quenching of a cross-linked phenylene vinylene polymer network was highly selective towards RDX vapors.[20] This sensing strategy can be used for the detection of RDX from solution or vapor phase.

Apart from traditional fluorescence methods, Förster (or fluorescence) resonance energy transfer (FRET) is a highly sensitive method.[21] FRET-based probes have exhibited excellent sensitivity, even to single molecule detection.[22, 23] Conventionally, the FRET-based chemosensors have been designed in the form of analyte-fluorophore pairs connected with a covalent linkage. These sensors are difficult to prepare and suffer from photo bleaching and the interference of environmental factors. To overcome these drawbacks, in recent years, traditional fluorescent dyes have been replaced with nanoparticles and quantum dots (QDs). The advantages of QDs include size tunable emission spectra covering from the UV to NIR regions, sharp emission signals, large stokes shifts, resistance to photo and chemical degradation and broad absorption windows.[24] For example, a FRET-based trinitrotoluene (TNT) sensor composed of CdTe/CdS core/shell QDs as the donor and a gold nanorod as the quencher showed very good selectivity.[25] Another work emphasized the use of a CdSe-ZnS core-shell QDs-antibody fragment in framing FRET-based TNT sensors.[26] Most of the FRET detection of explosives designed so far involves the detection of nitro-aromatic compounds, such as TNT and DNT. However, FRET-based fluorescent nanosensors for the detection of PETN are seldom found in the literature. This may be due to the inability of these explosives to quench the fluorescence emission through π- π interactions.

Herein, we report a novel FRET-based nanosensor system for the selective detection of PETN and RDX. The sensor is composed of diphenylamine (DPA) as the donor and cadmium sulfide quantum dots (CdS QDs) as the acceptor. In the QD-DPA system, the inherent fluorescence of DPA was quenched by resonance energy transfer to the CdS QDs. With the introduction of the explosive molecule (PETN or RDX), the interaction of DPA and the CdS QDs was broken, thereby forming a DPA-PETN complex. Hence the DPA fluorescence was restored. Plenty of reports are available in which semiconductor QDs act as the donor system and an organic dye acts as an acceptor. However, only a few publications have

shown that CdS QDs can act as an acceptor in FRET.[27-29] The present study demonstrated that CdS QDs can act as an effective acceptor in resonance energy transfer, which has been confirmed by steady state and time-resolved fluorescence measurements. The detection can be performed either by observing the turn-on of DPA fluorescence or by following the turn-off of resonance energy transfer. This provides an opportunity to follow the detection in two ways so the chance of false detection is greatly reduced. The probe offers high sensitivity towards PETN and RDX. The detection limit of PETN and RDX was found to be 10 nM and 20 nM, respectively. For the in situ analysis, an easy sampling method using a Teflon cloth was performed. Compared to TNT detection, literature available on highly effective detection of PETN is very few in number. To the best of our knowledge, this is the first report showing a FRET-based CdS QD sensor for PETN and RDX detection with a very high selectivity and a remarkable sensitivity.

Experimental

Details of materials and methods are given in the ESI† S1. 3-Mercaptopropanoic acid (MPA) capped CdS QDs were prepared according to the previously described procedure.[30] Briefly, 0.175 mM $CdCl_2.H_2O$ was mixed with 0.289 mM thiourea in 14 mL of deionized water. A 0.395 mM, 20 mL aqueous solution of MPA was added to the above mixture, and the pH of the resulting solution was adjusted to 10 using a 1 M NaOH solution. An aliquot of the resulting solution, 10 mL, was transferred to a 20 mL Teflon lined stainless steel autoclave, and it was maintained at 100 °C for 2 h before being cooled to room temperature. The absorption spectrum of the prepared CdS QDs shows a peak at 410 nm, which corresponds to ~4 nm size QDs[31] (see Fig. 1). Dynamic light scattering (DLS) studies and transmission electron microscopy (TEM) images support that size distribution of the QD are in the 4–5 nm range (see Fig. S2 in the ESI†). The prepared CdS QD solution was centrifuged, the residue was re-dispersed in deionized water and the pH of the solution was adjusted to 10. This solution was used for all further studies.

Results and discussion

The choice of DPA for the present sensor system was made carefully because of the following reasons. (i) DPA is highly selective towards nitroesters and nitramines.[32] (ii) The amine group of DPA can bind sufficiently strongly with the carboxylate group of the MPA ligand of the QD, leading to a strong donor –acceptor interaction. (iii) It has a sufficiently high fluorescence emission in the region of 330 – 430 nm (see Fig. S3 in the ESI†). The absorption wavelength of acceptor (CdS QD) is in the range of 350 – 440 nm (Fig. 1). The calculated J_{DA} value indicated a good spectral overlap between the donor and the acceptor (see inset of Fig. 2 for the spectral overlap and S10 in the ESI† for the calculation). No report has demonstrated the use of DPA as a fluorescent probe for the detection of PETN and RDX.

However, indirect fluorescence detection has been reported with diphenylamine derivatives.[17] In this work, NO_x species, a photofragmentation product of RDX/PETN, selectively react with newly developed dihydroacridines, which results in an increased fluorescence emission.

The intrinsic emission of CdS QDs shows a maximum at ~585 nm (Fig. 1). Various concentrations of DPA in ethanol were added to the CdS QD solution, and it was found that 250 µL of 100 nM DPA solution was able to provide a sufficiently good FRET emission at 585 nm (Fig. 2, trace (b)). See Fig. S4 in the ESI† for the variations in FRET intensity with respect to DPA concentration. The term 'CdS QD-DPA sensor system' or simply 'sensor system' is used in later parts of the text to represent the sensor solution containing 3 mL of CdS QD and 250 µL of 100 nM DPA. The UV-visible spectrum of CdS QD-DPA shows a 4 nm shift indicate the interaction between QD and DPA. The excitation wavelength was fixed at 280 nm, and both the excitation and emission slit width was 5 nm for all FRET studies. The fluorescence measurements were performed immediately after adding the analyte solution.

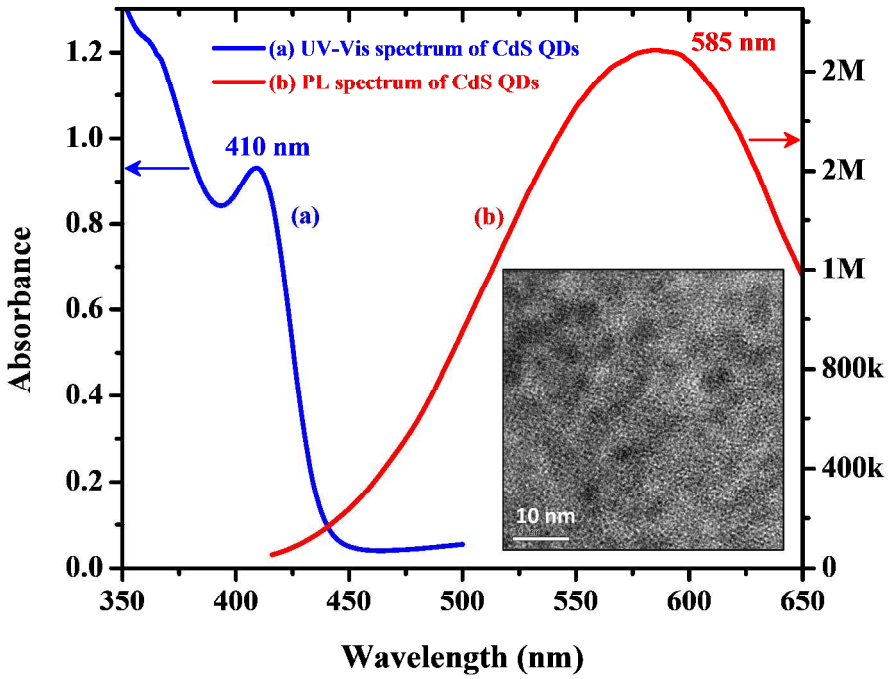

Fig. 1. (A) Absorption and emission spectra of CdS QDs; excitation wavelength was fixed at 410 nm. Inset shows the TEM image of CdS QD.

Fig. 2 demonstrates the FRET of the CdS QD-DPA system. Trace (a) in Fig. 2 represents the fluorescence spectrum of the CdS QD solution at 280 nm excitation, where a little emission is detected. Though the CdS QD is having an absorption tail that covers 280 nm, an excitation at 280 nm did not generate an appreciable emission from the QD. Whereas, 280 nm excitation of the CdS QD-DPA sensor

system (trace (b) in Fig. 2) result a significant emission centered at 585 nm. The strong fluorescence emission of DPA at 360 nm (See Fig. S3 in the ESI†, trace (b)) was quenched due to the resonance energy transfer. The emission from the acceptor (CdS QD) at the excitation wavelength indicates an efficient energy transfer between the donor and the acceptor. The details of the donor-acceptor interaction are discussed later.

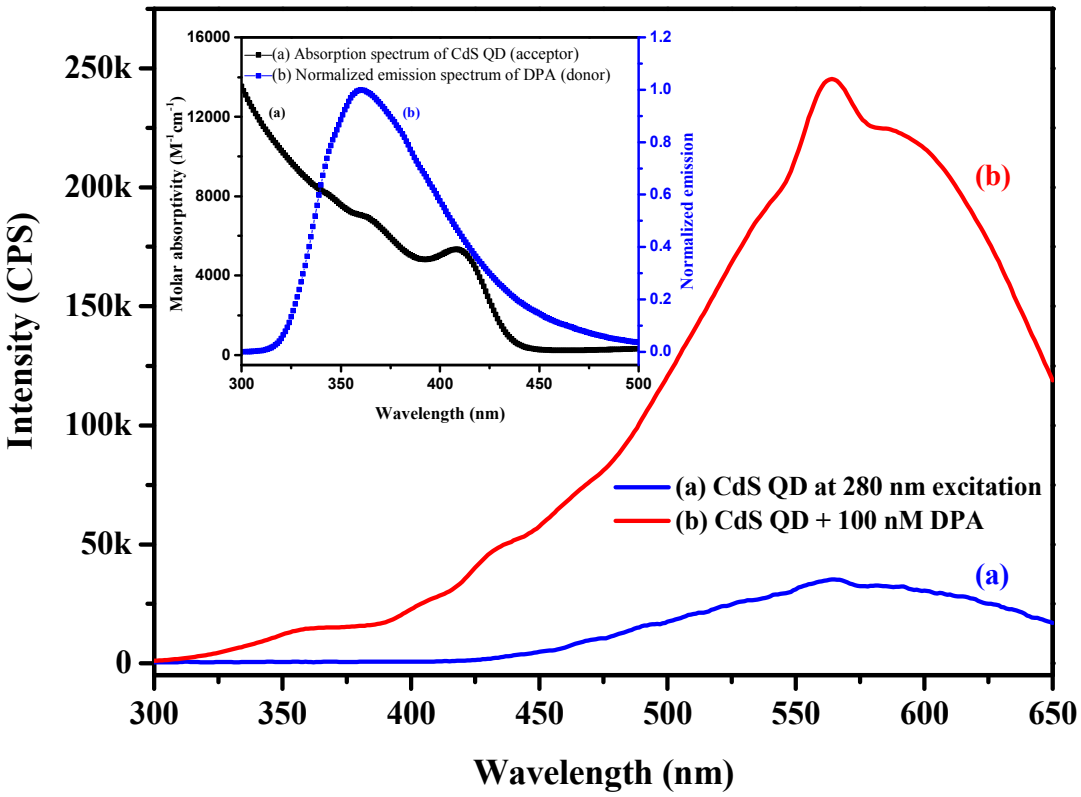

Fig. 2. Demonstration of FRET: fluorescence spectrum of (a) CdS QDs and (b) the CdS QD-DPA system at 280 nm excitation. A sharp peak at 560 nm is due to the second-order transmission through the emission monochromator.[33] *Inset*: emission spectrum of DPA and absorption spectrum of CdS QDs plotted together to show the spectral overlap between the donor and acceptor.

We will now discuss the detection of PETN using the CdS QD-DPA sensor system. Fig. 3 represents the fluorescence spectra of the CdS-DPA system with the addition of PETN. A series of concentrations of PETN was added to the sensor system. It is clear from the figure that addition of the PETN solution, with the resultant concentration of 10 nM, was able to produce a detectable change in the FRET (at 585 nm) and the inherent emission of DPA at 355 nm. The results of the addition of up to a 100 nM concentration of PETN are shown in Fig. 3. Clearly, we can observe the reduction in FRET intensity at 585 nm and fluorescence recovery of DPA at 355 nm. This response can be utilized for detection

purposes. These results can be attributed to (i) the strong electrostatic interaction between the non-bonded electrons of the >NH group of DPA and the positively charged nitrogen atoms of PETN,[34] leading to the increased acceptor–donor distance, and (ii) the repulsive interaction between the negatively charged nitro group of PETN and carboxylate group of the MPA ligand of the QDs that leads to the expulsion of the DPA-PETN pair from the CdS QDs. These factors affect the resonance energy transfer and result in turn-off of the FRET process and turn-on of the DPA emission at 355 nm. The fluorescent emission of pure DPA was 360 nm, but it is shifted to 355 nm due to the interaction with PETN. The peaks that appear at 405 nm and 430 nm are attributed to unreacted thiourea and 3-mercaptopropanoic acid, respectively.

As already indicated, one can perform explosive detection either by following the fluorescence recovery (turn-on) of DPA or observing the reduction (turn-off) in FRET intensity. A significant recovery (~70%) of DPA fluorescence was observed upon the addition of 100 nM PETN and emission due to FRET was almost absent. Within experimental error, ~10 nM PETN can be effectively detected under normal conditions. In an earlier report, an NADH analogue, 10-methyl-9,10-dihydroacridine, was employed for the detection of PETN and RDX. The detection limit was found to be 1.3×10^{-4} M and 7×10^{-5} M, respectively.[35] DPA is being used in the colorimetric detection of nitroester explosives.[36] The detection limit of the colorimetric method was 0.7 μg and 1 μg for nitrocellulose and nitroglycerine, respectively. The colorimetric determination of PETN and RDX using a fluorescent nanofiber was reported as having a detection limit of 7 ppt and 5 ppt, respectively.[37] In the present case, the detection limit is 10 nM (or 3200 pg). Therefore, our system is notably superior and reliable compared to other reported methods. In another report, where the indirect detection of PETN was achieved using a photo-fragmentation reaction, the detection limit was 320 pg, whereas in the present case, it is ~3200 pg.[17]

We tested simple bi-molecular systems containing DPA as the donor for the detection of explosives. The motivation was to check whether the alternative simple organic molecule could function as an acceptor in the DPA-based sensor dyad. For example, instead of CdS QDs, we used pyrene butyric acid as the acceptor. However, FRET process was not observed. This indicated that the selection of the acceptor was critical for PETN and RDX detection. CdS QDs may be a unique choice, and the photostability of this system is an added advantage for real applications. We also examined the fluorescence response of DPA-PETN system and no fluorescence change was observed. To check the influence of dilution in the sensor system's fluorescence, equivalent amount of ethanol solution (without PETN) was added. No apparent change in fluorescence was noticed.

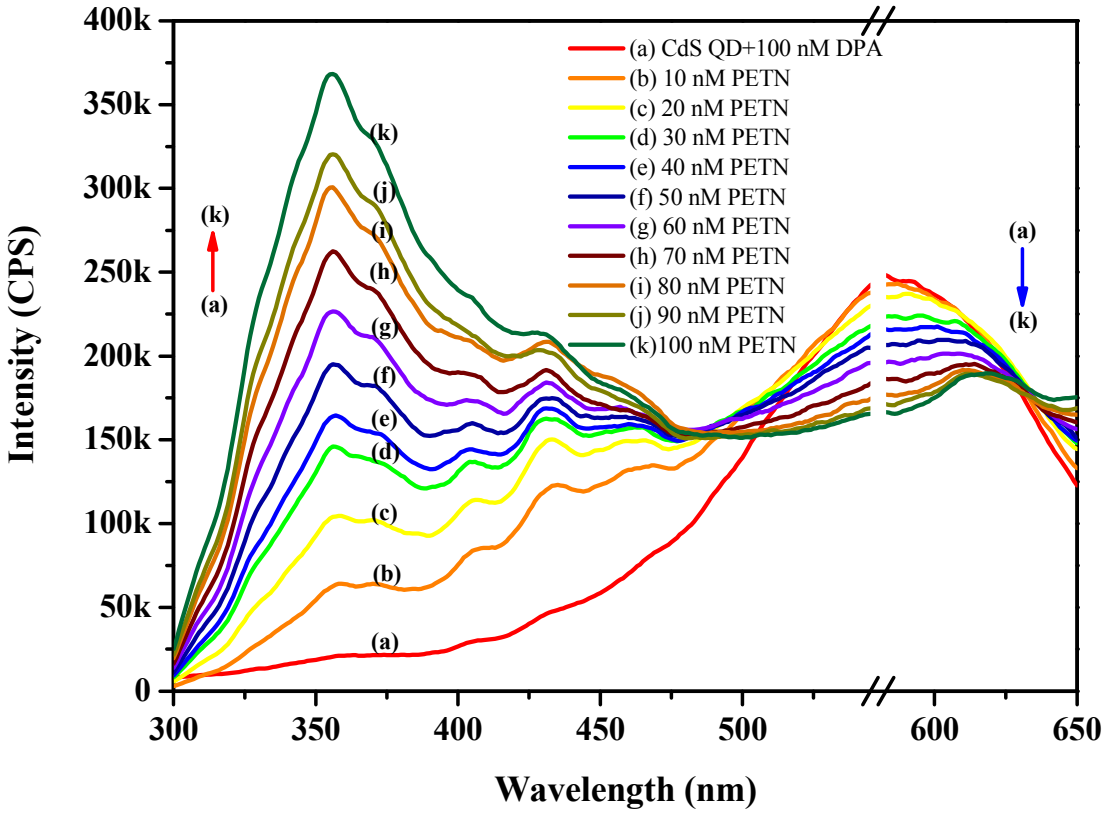

Fig. 3. Detection of PETN: Various concentrations (traces b-k) of PETN were added to the CdS QD-DPA system. Trace (a) represents the fluorescence spectrum of the CdS QD-DPA system. An increase in emission at 355 nm and a decrease in the FRET emission at 585 nm are observed. The wavelength region 545 nm - 580 nm (second-order transmission through the emission monochromator) is omitted from the figure for clarity.

The capability of the present sensor system for the detection of other explosives was verified. It is found that RDX, another destructive plastic explosive, also respond in a similar fashion. As in the PETN case, we added various concentrations of RDX to the CdS QD-DPA sensor system and followed both the FRET emission and fluorescence recovery (Fig. S5 in the ESI†). Overall, the observations were similar with slightly less detection limit. A detectable difference in FRET and fluorescence was observed upon the addition of 20 nM of RDX. The higher sensitivities for PETN, compared RDX detection may be attributed to the number and nature of nitro groups. Compared to PETN, the level of fluorescent recovery with respect to the concentration was lower. Approximately 60-65% of the DPA fluorescence was recovered with the addition of 200 nM of RDX.

The selectivity of the sensor system was tested for various molecules with functional groups, such as amines, carboxylic acids and nitro groups. Fig. 4 shows the result of the selectivity studies. The

selection of these compounds was made to include aliphatic and aromatic functional groups and structurally similar compounds. Interestingly, no substantial changes in FRET or fluorescence were observed (see Fig. 4 for the comparison of emission intensity at 355 nm). This indicates that these molecules are unable to break the CdS QD-DPA system. It should be noted that the spectra given in Fig. 4 is of the 1000 nM concentration of these analyte are comparing with 100 nM concentration of PETN and RDX. In addition to the individual analyte solutions, a mixture containing aniline-acetic acid, nitrobenzene-ethylenediamine, 2,4-dinitrophenol-benzoic acid and phenol-PETN was tested. Only the mixture containing PETN showed the turn-on of DPA fluorescence and reduction in FRET intensity. Therefore, it is clear that the present sensor system is highly selective towards PETN or RDX. Reproducibility and repeatability of the CdS QD-DPA sensor system has been tested with various batches of sensor system. The fluorescence response to PETN/RDX was always reproducible.

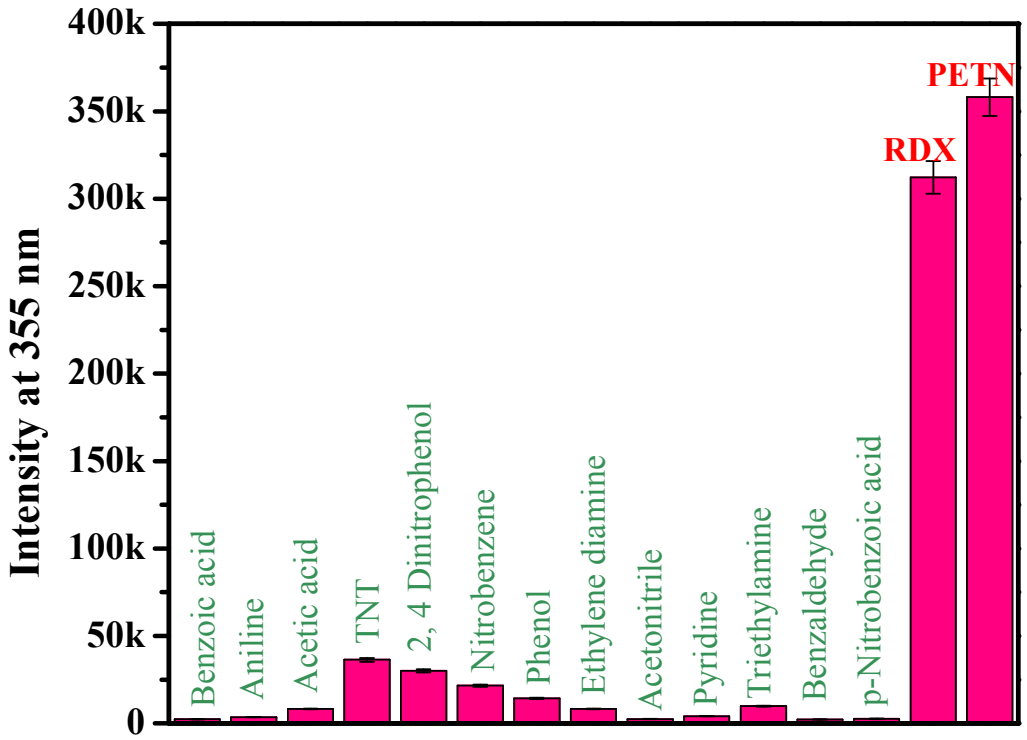

Fig. 4. Comparison of the turn-on intensity at 355 nm emission for various analytes. None of the analytes used for selectivity studies shows appreciable emission at 355 nm. Note that the comparison is made for the 1000 nM concentration of the above mentioned analytes with that of 100 nM PETN and RDX. Each data point is an average of three different experiments.

To evaluate practical applications, we demonstrated the use of a Teflon wiping substrate for the effective sampling of explosives from various surfaces. For example, the results of samplings from a leather surface are given in Fig. S6 in the ESI†. Various concentrations of PETN (200 μL) were drop-

casted on a leather surface and allowed to dry. A 2 cm x 2 cm Teflon cloth wetted with ethanol was used as a wiping substrate. After swabbing the surface, the cloth was folded carefully and placed in the quartz cuvette containing 3 mL of the CdS QD-DPA sensor system. The cuvette was then subjected to gentle shaking for 10 seconds. Subsequently, the fluorescence measurements have been done. Proper care was taken when placing the cloth in the cuvette to avoid the path of the light source and the detector. It was observed that sampling from a dried spot of 50 nM of PETN was able to produce detectable changes in the fluorescent spectrum. We believe that this easy in situ sampling method can be highly effective in explosive detection at security check points. The procedure is not kinetically controlled. We repeated the fluorescence measurement in every 10 min for 1 hr. No change in fluorescence was observed during this time scale.

There are very few reports available for CdS QDs as the acceptor in a FRET system. This is mainly due to the long life time of QDs.[38, 39] Fluorescence life time measurements of donor and acceptor systems are given in Fig. S7 in the ESI†. The time-resolved fluorescence spectra of the donor (DPA) alone and in the presence of the acceptor (CdS QDs) support the existence of the FRET process. It is clear that the donor decay is significantly decreased in the presence of the acceptor. The photoluminescence decay time of the donor (DPA) was a double exponential fit with lifetimes of 17.849 ns and 2.7935 ns and an average lifetime of 11.35 ns. The average lifetime was calculated using the previously described equation $<\tau>= (a_1 \tau_1+ a_2 \tau_2+ a_3 \tau_3)$ (ns).[40] The pre-exponential factors were 0.5686 and 0.4314 for the long-lived component and short-lived component, respectively. The existence of two different decay times for DPA can be attributed to the existence of molecular forms: (a) an un-conjugated and (b) a conjugated form, eventually giving two different decay times (See Fig. S8 in the ESI†). The existence of two molecular forms is supported by solution phase infrared spectroscopy. The C-N stretching vibration is split into two and observed at 1307 and 1317 cm^{-1}. The labile nature of hydrogen can impart a double bond character to one of the C–N bonds of DPA and result in a peak split for C–N stretching vibrations.

After the addition of the acceptor (CdS QDs), the lifetime of donor was decreased significantly and has been averaged to 7.06 ns. We assumed that the interaction of the CdS QDs with the donor decreases the lifetime with a subsequent shift in the equilibrium towards the left. The decay time of the donor in the presence of the acceptor was a 3 exponential fit with lifetimes of 3.665 ns, 21.80 ns and 0.43 ns, having pre-exponential factors of 0.2771, 0.2684 and 0.4545, respectively. The details of the fitting parameters and lifetime values are given in Table 1. Owing to the strong dipole-dipole interaction between the donor (DPA) and the acceptor (CdS QD) and due to high spectral overlap, the FRET probe manifested a fairly good FRET efficiency (E_{D-A}) of 45%, which was calculated using the steady state fluorescence data.[25] The

value of FRET efficiency was also used to calculate the theoretical distance between the donor and the acceptor, which was found to be 4.39 nm. See S10 in the ESI† for calculations.

Table 1. Time-resolved fluorescence data of the donor (DPA) in the absence and presence of the acceptor

System	τ_1(ns)	a_1	τ_2(ns)	a_2	τ_3(ns)	a_3	χ^2	$<\tau>=(a_1\tau_1+a_2\tau_2+a_3\tau_3)$ (ns)
DPA	2.7935	0.4314	17.849	0.5686	-	-	1.7477	11.35
DPA + CdS QD	3.665	0.2771	21.80	0.2684	0.43	0.4545	1.1827	7.06

The fairly good FRET efficiency of 45% for the sensor system is mainly attributed to two factors. First, as the FRET efficiency is inversely proportional to sixth power of the distance between the donor and the acceptor, a short thiol-molecule, such as MPA, is important, as its length falls below 0.5 nm.[25] Additionally, the pKa value of MPA is 4.3,[41] and at the experimental pH 10, almost complete ionization of the carboxyl group leads to the formation of carboxylate ions. This facilitates the strong electrostatic interaction with the amine group of DPA, placing the donor and acceptor in close vicinity. Second, there is a good spectral overlap between the emission spectrum of the donor and excitation spectrum of the acceptor molecules, as indicated by the calculated J_{DA} = 1.086e+14 nm^4/(M*cm).

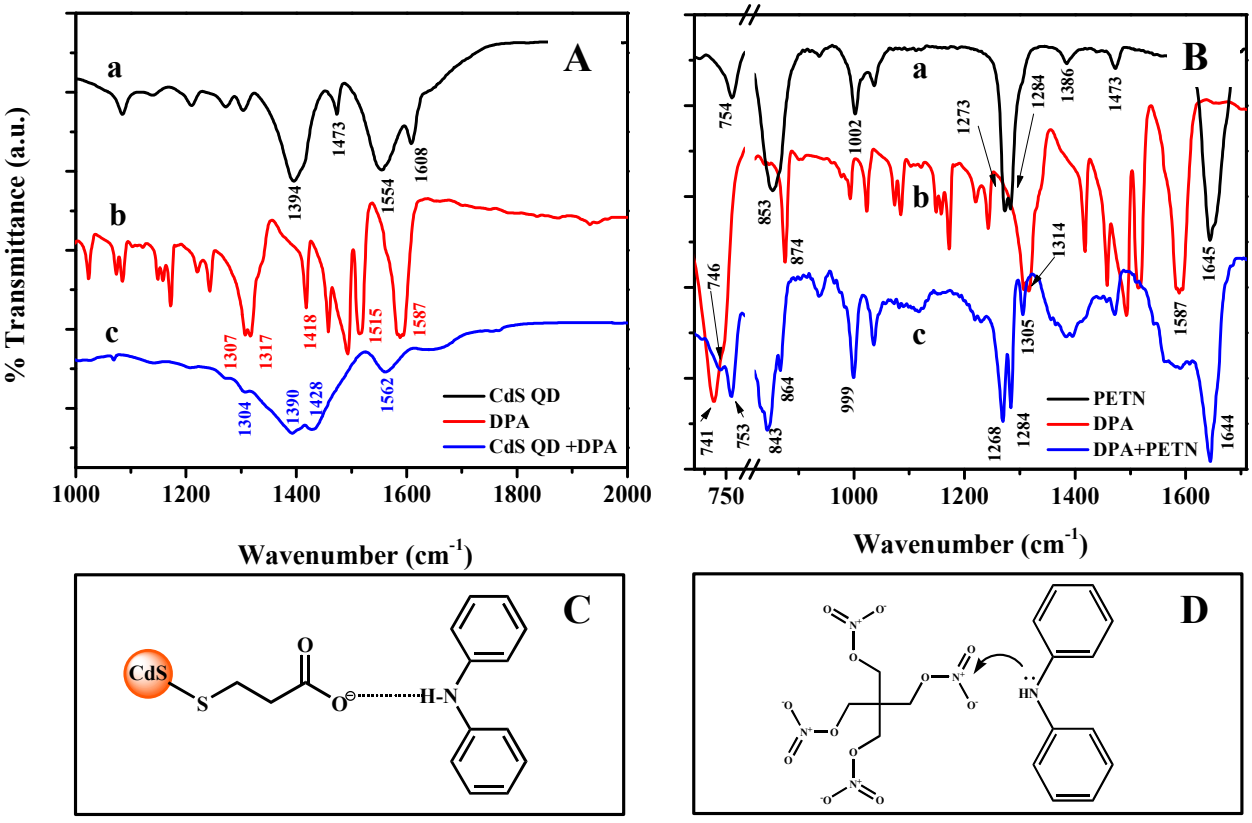

Fig. 5. (A) show the infrared spectra of CdS QDs (trace a), DPA (trace b) and the CdS QD-DPA sensor system (trace c). (B) show the infrared spectra of PETN (trace a), DPA (trace b) and the DPA-PETN mixture (trace c). The plausible interaction between (C) CdS-QD and DPA (D) PETN and DPA are also shown.

We conducted a detailed investigation on the interactions between CdS QDs, DPA and PETN using infrared spectroscopy (Fig. 5). In Fig. 5A, trace (a), the strong absorption bands at 1554 cm^{-1} and 1394 cm^{-1} are attributed to the asymmetric and symmetric stretching vibrations of the MPA carboxylate group, respectively.[42, 43] The absence of a peak approximately 1700 cm^{-1} in the spectrum indicates the complete ionization of the carboxyl group to carboxylate at the present experimental pH of 10. The peak at 1608 cm^{-1} could be the interference of the water's –OH bending vibrations. After the addition of DPA to the CdS QDs (Fig. 5A, trace c), the asymmetric stretching vibration of the carboxylate group experienced a significant blue shift; the original peak at 1554 cm^{-1} is shifted to 1562 cm^{-1} (Fig. 5A, trace (c)). This is due to the formation of a strong hydrogen bonding interaction between the carboxylate group of the CdS QDs and the >NH group of DPA. Due to the hydrogen bonding interaction, the resonance contribution of the negatively charged oxygen atom is restricted. This in turn strengthens the >C=O vibration of the carboxylate group by imparting more double bond character. Similarly, in the case of pure DPA, the strong absorptions at 3383 cm^{-1} and 3407 cm^{-1}, which are due to the N-H stretching of DPA,[44] now appeared as a broad band centered at 3330 cm^{-1} (see ESI† S9, Fig. (A)). This weakening of the N-H stretching vibrations supports the existence of a hydrogen bonding interaction between DPA and the carboxylate group of the MPA ligand (See Scheme D in Fig. 5).

Now, we will discuss the interaction of PETN with that of DPA (Fig. 5B). Two types of interactions could be expected between DPA and PETN: (a) hydrogen bonding interaction between the >NH group of DPA and the negatively charged O atoms of PETN and (b) interaction between the positively charged N atom of the PETN and the lone pair electrons of the N atom of DPA. Previous reports reveal that the latter is more pronounced due to the strong electron repelling nature of the amino group and the electron attracting nature of the nitro group.[23] Our infrared studies also suggest the existence of the second possibility. Note that we have presented the infrared spectrum of the DPA-PETN pair because the infrared spectrum of the CdS QD-DPA-PETN system is very broad and vague. The infrared peak assignments of PETN were performed according to reference 44. The discussion of molecular interaction is given in the ESI† S9. From the infrared spectroscopy evidence, we suggest that in the DPA-PETN pair, (i) the O–NO_2 bending vibration is weakened, (ii) the NO_2 bond strength is unaffected, (iii) the C–O and –O–N stretching are weakened, and (iv) the NH_{wag} (bending) becomes stronger. This could result only from the interaction between the positively charged N of PETN and the

lone pair of the N from DPA. If the interaction is via the H of >NH group (of DPA) and the negatively charged O atoms of PETN, then we should expect a difference in the NO_2 stretching vibrations and an unaffected C–O and O–N bond in PETN.

Conclusions

We successfully demonstrated the use of a CdS QD-DPA sensor system for the selective detection of high explosives, such as PETN and RDX. The detection limit of the sensor system for PETN and RDX was found to be 10 nM and 20 nM, respectively. In a typical detection procedure, we can follow either the decrease in the FRET intensity at ~585 nm or the evolution of fluorescence at ~355 nm. The success of the sensor system can be attributed to the selectivity of DPA towards PETN and RDX. The selectivity of the sensor system was tested for various functional groups, such as amines, carboxylic acids, phenols, and nitro groups. The response by FRET or the fluorescence recovery of DPA was not observed for these analytes. In situ sampling and detection of analyte from leather surface were demonstrated using a Teflon wiping cloth, though the detection limit was found to be one order less. The nature of the interactions between DPA, CdS QDs and analytes was established using infrared spectroscopy. CdS QDs interact with DPA via hydrogen bonding, and the DPA-PETN interaction was through the lone pair electrons of the N atom of DPA and the positively charged N atom of the PETN.

The present report is the first FRET-based CdS QD sensor for selective detection of explosives PETN and RDX. Although plenty of reports are available on fluorescent detection of nitroaromatic explosives, such as TNT and DNT, demonstrations of selective detection of nitrate esters, such as PETN, are very few in number. The detection limit of the CdS QD-DPA sensor system was 10 nM (3200 pg) for PETN detection and is better than many reported methods. The turn-on and turn-off response provides an added advantage of pursuing detection in a two-way manner and reduces erroneous detection. The easy one pot synthesis method of CdS QDs and use of cheap and readily available chemicals make the present sensor system cost effective. Excellent selectivity and high sensitivity of the sensor system make it attractive for practical applications in airports and other security check points.

Acknowledgements

Authors thank IIST for the financial support. We acknowledge Vikram Sarabhai Space Centre Thiruvananthapuram for providing PETN, RDX and TNT. We acknowledge DST Unit on Nanoscience at IIT Madras and IISER, Thiruvananthapuram for materials characterization.

References

1. R. G. Ewing, B. H. Clowers and D. A. Atkinson, *Anal. Chem.*, 2013, **85**, 10977–10983.
2. K. M. Roscioli, E. Davis, W. F. Siems, A. Mariano, W. Su, S. K. Guharay and H. H. Hill, *Anal. Chem.*, 2011, **83**, 5965-5971.
3. J. Maggie Tam and Herbert H. Hill, *Anal. Chem.*, 2004, **76**, 2741-2747.
4. S. Botti, S. Almaviva, L. Cantarini, A. Palucci, A. Puiu and A. Rufoloni, *J. Raman Spectrosc.*, 2013, **44**, 463-468.
5. S. S. R. Dasary, A. K. Singh, D. Senapati, H. Yu and P. C. Ray, *J. Am. Chem. Soc.*, 2009, **131**, 13806-13812.
6. A. Mathew, P. R. Sajanlal and T. Pradeep, *Angew. Chem. Int. Ed.*, 2012, **51**, 9596-9600.
7. Y. Peng, A.-J. Zhang, M. Dong and Y.-W. Wang, *Chem. Commun.*, 2011, **47**, 4505-4507.
8. E. S. Forzani, D. Lu, M. J. Leright, A. D. Aguilar, F. Tsow, R. A. Iglesias, Q. Zhang, J. Lu, J. Li and N. Tao, *J. Am. Chem. Soc.*, 2009, **131**, 1390-1391.
9. M. Y. Ho, N. D'Souza and P. Migliorato, *Anal. Chem.*, 2012, **84**, 4245-4247.
10. I. Cotte-Rodríguez, Z. Takáts, N. Talaty, H. Chen and R. G. Cooks, *Anal. Chem.*, 2005, **77**, 6755-6764.
11. J. F. Garcia-Reyes, J. D. Harper, G. A. Salazar, N. A. Charipar, Z. Ouyang and R. G. Cooks, *Anal. Chem.*, 2010, **83**, 1084-1092.
12. E. V. K. G. A. Eiceman , and N. S. Krylova, *Anal. Chem.*, 2004, **76**, 4937–4944.
13. T. Demeritte, R. Kanchanapally, Z. Fan, A. K. Singh, D. Senapati, M. Dubey, E. Zakar and P. C. Ray, *Analyst*, 2012, **137**, 5041-5045.
14. C. Muthu, S. R. Nagamma and V. C. Nair, *RSC Advances*, 2014, **4**, 55908-55911.
15. R. C. Stringer, S. Gangopadhyay and S. A. Grant, *Anal. Chem.*, 2010, **82**, 4015-4019.
16. Y. Salinas, R. Martinez-Manez, M. D. Marcos, F. Sancenon, A. M. Costero, M. Parra and S. Gil, *Chem. Soc. Rev.*, 2012, **41**, 1261-1296.
17. T. L. Andrew and T. M. Swager, *J. Org. Chem.*, 2011, **76**, 2976-2993.
18. Y. Ma, H. Li, S. Peng and L. Wang, *Anal. Chem.*, 2012, **84**, 8415-8421.
19. B. Dedeoglu, A. Monari, T. Etienne, V. Aviyente and A. S. Özen, *J. Phys. Chem. C*, 2014, **118**, 23946-23953.
20. D. Gopalakrishnan and W. R. Dichtel, *J. Am. Chem. Soc.*, 2013, **135**, 8357-8362.
21. G. Chen, F. Song, X. Xiong and X. Peng, *Ind. Eng. Chem. Res.*, 2013, **52**, 11228-11245.
22. R. Roy, S. Hohng and T. Ha, *Nat Meth*, 2008, **5**, 507-516.
23. W. Bae, M.-G. Choi, C. Hyeon, Y.-K. Shin and T.-Y. Yoon, *J. Am. Chem. Soc.*, 2013, **135**, 10254-10257.
24. X. Wang, J. Zheng, X. Sui, H. Xie, B. Liu and X. Zhao, *Dalton Trans.*, 2013, **42**, 14726-14732.
25. Y. Xia, L. Song and C. Zhu, *Anal. Chem.*, 2011, **83**, 1401-1407.
26. E. R. Goldman, I. L. Medintz, J. L. Whitley, A. Hayhurst, A. R. Clapp, H. T. Uyeda, J. R. Deschamps, M. E. Lassman and H. Mattoussi, *J. Am. Chem. Soc.*, 2005, **127**, 6744-6751.
27. H. Xu, X. Huang, W. Zhang, G. Chen, W. Zhu and X. Zhong, *ChemPhysChem*, 2010, **11**, 3167-3171.
28. G. Jiang, A. S. Susha, A. A. Lutich, F. D. Stefani, J. Feldmann and A. L. Rogach, *ACS Nano*, 2009, **3**, 4127-4131.
29. A. R. Clapp, I. L. Medintz and H. Mattoussi, *ChemPhysChem*, 2006, **7**, 47-57.
30. A. Aboulaich, D. Billaud, M. Abyan, L. Balan, J.-J. Gaumet, G. Medjadhi, J. Ghanbaja and R. Schneider, *ACS Appl. Mater. Interfaces*, 2012, **4**, 2561-2569.
31. W. W. Yu, L. Qu, W. Guo and X. Peng, *Chem. Mater.*, 2003, **15**, 2854-2860.
32. T. C. Thanarachatapoom, N.; Wilairat, P., *Proceedings of the 2nd ASEAN Plus Three Graduate Research Congress (2ndAGRC), Bangkok*, February 2014.
33. J. R. Lakowicz, *Principles of Fluorescence spectroscopy*, 3rd edn., springer publishers, 2006.
34. T. Urbański, *Tetrahedron*, 1959, **6**, 1-9.

35. T. L. Andrew and T. M. Swager, *J. Am. Chem. Soc.*, 2007, **129**, 7254-7255.
36. P. K. Walker and P. J. Rodacy, *SANDIA REPORT*, January 2002.
37. A. L. Ying Wang , Yu Ding , Yixin Liu , and Yu Lei, *Adv. Funct. Mater.* , 2012, **22**, 3547-3555.
38. A. R. Clapp, I. L. Medintz, B. R. Fisher, G. P. Anderson and H. Mattoussi, *J. Am. Chem. Soc.*, 2005, **127**, 1242-1250.
39. S. Ast, P. J. Rutledge and M. H. Todd, *Phys. Chem. Chem. Phys.*, 2014, **16**, 25255-25257.
40. T. Sen and A. Patra, *J. Phys. Chem. C*, 2008, **112**, 3216-3222.
41. X. W. Lin, C.; Xu, S.; Cui, Y., *J. Phys. D: Appl. Phys.*, 2014, **47**.
42. S. E. Cabaniss and I. F. McVey, *Spectrochim. Acta, Part A*, 1995, **51**, 2385-2395.
43. I. Hocaoglu, M. N. Cizmeciyan, R. Erdem, C. Ozen, A. Kurt, A. Sennaroglu and H. Y. Acar, *J. Mater. Chem.*, 2012, **22**, 14674-14681.
44. K. A. Rajarajan, A.; Reka, D. KR.; Madhuramba, G., *J Pharm Chem Biol Sci*, 2013, **3**, 480-487.

Table of Content Figure